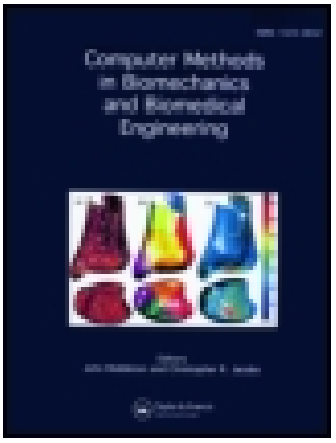

Computer Methods in Biomechanics and Biomedical Engineering

Publication details, including instructions for authors and subscription information:
http://www.tandfonline.com/loi/gcmb20

# A new stent with streamlined cross-section can suppress monocyte cell adhesion in the flow disturbance zones of the endovascular stent

Zengsheng Chen[ab], Fan Zhan[c], Jun Ding[bd], Xiwen Zhang[a] & Xiaoyan Deng[c]

[a] Department of Engineering Mechanics, School of Aerospace, Tsinghua University, 100084 Beijing, P.R. China

[b] Artificial Organs Laboratory, Department of Surgery, University of Maryland School of Medicine, Baltimore, MD 21201, USA

[c] Key Laboratory for Biomechanics and Mechanobiology of Ministry of Education, School of Biological Science & Medical Engineering, Beihang University, 100191 Beijing, P.R. China

[d] Department of Mechanical Engineering, University of Maryland, Baltimore County, Baltimore, MD 21250, USA

Published online: 01 Dec 2014.

To cite this article: Zengsheng Chen, Fan Zhan, Jun Ding, Xiwen Zhang & Xiaoyan Deng (2014): A new stent with streamlined cross-section can suppress monocyte cell adhesion in the flow disturbance zones of the endovascular stent, Computer Methods in Biomechanics and Biomedical Engineering, DOI: 10.1080/10255842.2014.984701

To link to this article: http://dx.doi.org/10.1080/10255842.2014.984701

*Computer Methods in Biomechanics and Biomedical Engineering*, 2014
http://dx.doi.org/10.1080/10255842.2014.984701



# A new stent with streamlined cross-section can suppress monocyte cell adhesion in the flow disturbance zones of the endovascular stent

Zengsheng Chen[a,b1], Fan Zhan[c1], Jun Ding[b,d], Xiwen Zhang[a]* and Xiaoyan Deng[c]*

[a]*Department of Engineering Mechanics, School of Aerospace, Tsinghua University, 100084 Beijing, P.R. China;* [b]*Artificial Organs Laboratory, Department of Surgery, University of Maryland School of Medicine, Baltimore, MD 21201, USA;* [c]*Key Laboratory for Biomechanics and Mechanobiology of Ministry of Education, School of Biological Science & Medical Engineering, Beihang University, 100191 Beijing, P.R. China;* [d]*Department of Mechanical Engineering, University of Maryland, Baltimore County, Baltimore, MD 21250, USA*

(*Received 10 May 2014; accepted 3 November 2014*)

We proposed a new stent with streamlined cross-sectional wires, which is different from the clinical coronary stents with square or round cross-sections. We believe the new stent might have better hemodynamic performance than the clinical metal stents. To test the hypothesis, we designed an experimental study to compare the performance of the new stent with the clinical stents in terms of monocyte (U-937 cells) adhesion. The results showed that when compared with the clinical stents, the adhesion of U-937 cells were much less in the new stent. The results also showed that, when Reynolds number increased from 180 (the rest condition for the coronary arteries) to 360 (the strenuous exercise condition for the coronary arteries), the flow disturbance zones in the clinical stents became larger, while they became smaller with the new stent. The present experimental study therefore suggests that the optimization of the cross-sectional shape of stent wires ought to be taken into consideration in the design of endovascular stents.

**Keywords:** restenosis; streamlined cross-section; monocytes; adhesion; endovascular stent



## Introduction

The restenosis in endovascular stents is an unsolved problem in clinics. It has been well documented that the initiation and progression of restenosis is often related to flow disturbance with low wall shear stress (WSS) and high oscillating shear index (OSI), which results from the structure of the stent (Berry et al. 2000; Thury et al. 2002; Benard et al. 2003; LaDisa et al. 2005; Seo et al. 2005; Hara et al. 2006; Balossino et al. 2008; Kolandaivelu et al. 2011; Hsiao, Chiu, et al. 2012; Hsiao, Lee, et al. 2012; Papafaklis et al. 2012). Local hemodynamics is very sensitive to the geometry and structure of a stent (Berry et al. 2000; Seo et al. 2005; Kolandaivelu et al. 2011; Papafaklis et al. 2012). Therefore, it had been recognized that the stent structure has a clear-cut impact on the outcomes of arterial stenting treatment, i.e., the restenosis rate varies with stent design and geometry (Sigwart et al. 1987; Rogers and Edelman 1995; Farb et al. 1999; Lansky et al. 2000; Kastrati et al. 2001; Gurbel et al. 2002; McLean and Eigler 2002).

Most clinical coronary stents consist of metal wires with cross-sections of square or round shape that can disrupt blood flow leading to flow separation and vortex formation with low WSS and high OSI (Mattos et al. 1999; Morton et al. 2004). The outline of a fish or air plan is streamlined which reduces their flow resistance. Inspired by this concept, we proposed to use metal wires with streamlined cross-sections in the design of endovascular stents and hypothesized that this kind of new stents could minimize flow disturbance, and as a result, suppress the progression of stent restenosis. Because the adhesion of circulating monocytes to vascular endothelial cells is an important event that accelerates the initiation and progression of restenosis (Henry and Chen 1993; Moreno et al. 1996; Rogers et al. 1996, 1998; Chiu and Chien 2011) and many studies have revealed that flow disturbance with flow separation and vortex formation facilitates the adhesion of monocytes (Pritchard et al. 1995; Barber et al. 1998), in the article, we designed an experimental study to compare the performance of the new stent with the clinical stents in terms of monocyte (U-937 cells) adhesion. The aim of the study is to test the aforementioned hypothesis.

## Materials and methods

### *Materials*

U-937 cells used in the experiment were obtained from Peking Union Medical College, which are monocyte-like cells and histiocytic lymphoma cell line (Sundström and Nilsson 1976). U-937 cells can produce the integrins of sLex, β1 and β2 so that their adhesion process with the

*Corresponding authors. Email: zhangxiw@tsinghua.edu.cn, dengxy1953@buaa.edu.cn

endothelial cells is similar to that of the monocytes (Gonzales and Wick 1996). Therefore, U-937 cell is a good model of monocytes in studying adhesion interactions with endothelial cells (Cybulsky and Gimbrone 1991; Beekhuizen et al. 1992; Hauser et al. 1993; Calderon et al. 1994).

Sylgard 184 silica gel was purchased from Dow Corning Co., Midland, MI, USA. E-selecting, bovine serum albumin (BSA), double resistance to penicillin, streptomycin, fetal bovine serum, phorbol-12-myristate-13-acetate (PMA), phosphate buffer (PBS), glutaraldehyde, were purchased from Sigma Chemical Co. (St Louis, MO, USA).

### *U-937 cells preparation*

The U-937 cells could be differentiated by vitamin D3, interferons γ, tumor necrosis factor, retinoic acid, and phorbol ester. Prior to the experiment, the U-937 cells were thawed. Then, they were vaccinated in RPMI1640 culture fluid that consisted of 10% fetal bovine serum, 100 U/ml streptomycin, and 100 U/ml penicillin and cultivated in the culture box at 37°C and 5% $CO_2$ for 3 or 4 days. The cell propagation was executed after cultivating.

### *The test tube*

The test tube with a length and inner diameter of 60 and 3 mm, respectively, was made of sylgard 184 that was a two-component transparent organic silica gel. The initial state of this silica gel is fluid that can be solidified and becomes a bouncy material by mixing the two components in a proportion of 10:1.

### *Stents preparation*

Five circular rings placed in the test silica gel tube were used to imitate endovascular stent deployed in an artery (Seo et al. 2005; Hsiao, Lee, et al. 2012). The rings were made of a photosensitive resin using laser rapid prototyping technique. For comparison, three types of rings with different cross-sections were used, namely square (Figure 1(A)), round (Figure 1(B)), and streamlined (Figure 1(C)). The diameter of the rings was 3 mm.

The streamlined cross-sectional ring has an outline curve (Figure 1(C)) that can be described by the following equation:

$$R(z) = 0.1e^{-z^2} \quad (-2.5 \le z \le 2.5), \tag{1}$$

where $z = d/h$, is the normalized axial coordinate.

Both the thickness ($d$) and height ($h$) of the rectangular and round rings were set as 0.2 mm that were similar to those of most clinical metal stents (Garasic et al. 2000; Morton et al. 2004; Seo et al. 2005). Correspondingly, the thickness ($d$) of the streamlined rings was set as 0.5 mm so that their height was 0.2 mm. The thickness of 0.5 mm was also in the range for the clinical stents (Rogers and Edelman 1995; Capelli et al. 2009). In Figure 1, the letter $L$ denotes the length of the flow recirculation zone distal to each stent ring, which is the distance from the flow separation point to the flow reattachment point.

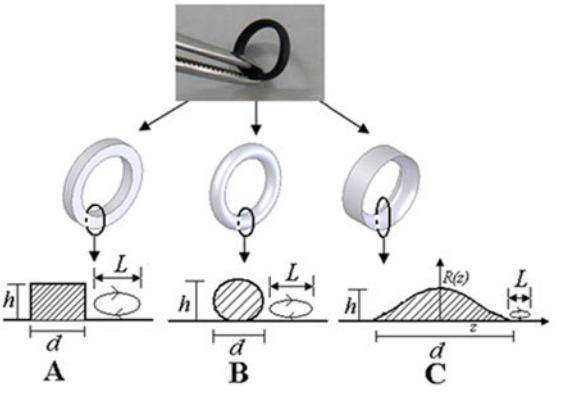


Figure 1. Picture of a representative circular ring stent and the sketch of the cross-sections of the three different rings used in the study. (A) Square cross-section, (B) round cross-section, and (C) streamlined cross-section. $d$, the thickness of the stent rings; $h$, the height of the rings; $L$, the length of the recirculation zones used to describe flow disturbance distal to each stent ring.

### *Experimental perfusion system*

The experimental perfusion system is illustrated in Figure 2, which consists of a head tank, a constant temperature water bath box, the test section of the stents, a downstream collecting reservoir, a peristaltic flow pump, and connecting latex tubes with an internal diameter of 3 mm. By altering the elevation of the head tank, the flow rate through the test section could be varied. The test section was the silica gel test tube deployed with five test circular rings imitating an endovascular stent. The test tube was perfused with a U-937 cells suspension.

In this comparative study, four experimental conditions were set up: (A) the silica gel test tube deployed with the square wire stents; (B) the silica gel test tube deployed with round wire stents; (C) the silica gel test tube deployed with streamlined wire stents; and (D) the silica gel test tube with no stents (as shown in Figure 2). The perfusion experiments were carried out for two Reynolds numbers. The low *Re* of 180 represents the rest condition of the coronary artery blood flow and the high one of 360 is for the strenuous exercise condition.

### *Experimental procedure*

For each experiment, five stent rings were equidistantly placed in the test tube and the interval between two rings

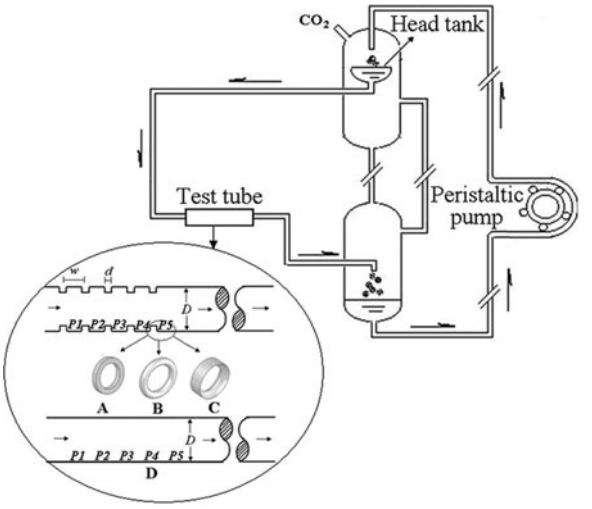


Figure 2. Schematic drawing of the perfusion system. The sketch at the lower left corner shows the four experimental conditions: (A) deployed with square wire stents; (B) deployed with round wire stents; (C) deployed with streamlined wire stents, and (D) deployed with no stents. *P*1 to *P*5 denotes the five disturbed flow zones distal to the five rings of the stent. For experimental condition D, the adhesion density of U-937 cells at the zones of *P*1 to *P*5 was counted for the comparison with experimental conditions A, B and C. *D*, the diameter of the test tube, which is 3 mm; *w*, the space between two adjacent rings, which is 1.0 mm; *d*, the thickness of the stent rings.

was 1 mm (Seo et al. 2005; Hsiao, Lee, et al. 2012). The test tube with or without the stent rings was first immersed in deionized water and then dried in air. The inner wall of the tube was coated with E-selectin of 3 μg/ml and placed in a refrigerator at 4°C for 20 h, then rinsed with PBS. Prior to the perfusion experiment, in order to avoid the nonspecific cellular adhesion of U-937, the test tube was blocked with 1% BSA in PBS for 1 h at 37°C. Then, the test tube was rinsed with PBS again.

The U-937 cells concentration of the perfusion suspension was adjusted to $5 \times 10^5$ platelets per milliliter. PMA with the concentration of 0.2 μg/ml was used to stimulate the U-937 cells to adhere to the E-selecting coated test tube.

During the experiment, the U-937 cells suspension was perfused though the test tube at room temperature for 3 h. Each experimental condition was repeated four times.

Immediately after the perfusion, the test tube was removed from the perfusion system and flashed with PBS. Then, the inner surface of the test tube was fixed with glutaraldehyde and put in the refrigerator at 4°C for 12 h.

After fixation, the test tube was dried and then observed with an inverted microscope (Olympus Optical Co., Ltd, Tokyo, Japan) to study the distribution of U-937 cells adhesion along the test tube by projecting the image of the adhering cells onto a computer display using a video camera (Olympus Optical Co., Ltd) connected to the computer.

### *Statistics*

The results of U-937 cells adhesion density observed were presented as means ± standard deviation. Statistical relevance was determined using analysis of *T*-test with *P* values below 0.05.

### *Flow characterization in the test section*

In order to characterize the flow pattern in the test section, numerical flow simulations were carried out, as shown in Figure 3.

The computational fluid was the experimental perfusion solution, that was simplified as an incompressible, homogeneous, Newtonian viscous fluid, with a density ($\rho$) of 1060 kg/m$^3$ and a constant viscosity ($\mu$) of $1.1 \times 10^{-3}$ kg/m s (Schmid-Schonbein 1987; Barber et al. 1998; Ng et al. 2002). At the two Reynolds numbers (180 and 360), the flow in the test tube should remain laminar. The boundary conditions were set as follows:

(1) A uniform velocity profile was assumed at the test tube inlet.
(2) The outlet condition was set to be outflow, which makes the flow at the outlet to be a fully developed flow.
(3) The wall of the test tube were assumed to be rigid and non-slip.

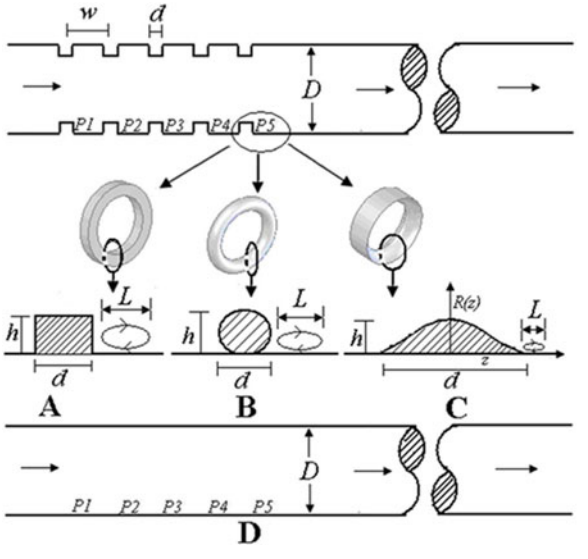


Figure 3. The four geometric models used in the flow simulations in the test tube. (A) Deployed with square wire stents; (B) deployed with round wire stents; (C) deployed with streamlined wire stents; and (D) deployed with no stents. *D*, the diameter of the test tube; *d*, the thickness of the wire rings; *h*, the height of the wire rings, which is 0.2 mm; *w*, the space between two adjacent rings, which is 1.0 mm; *L*, the length of recirculation zone (vortex) distal to each stent ring, the disturbed flow zone distal to each ring is denoted by *P*1 to *P*5.

The numerical simulations were based on the three-dimensional incompressible Navier–Stokes equations as follows:

$$\rho(\vec{u}\cdot\nabla)\vec{u} + \nabla p - \mu\Delta\vec{u} = 0, \quad (2)$$

$$\nabla\cdot\vec{u} = 0, \quad (3)$$

where $\vec{u}$ is the fluid velocity vector, $\rho$ and $\mu$ are the density and viscosity of fluid, and $p$ the pressure.

Finite volume method was used in the simulation. The computational meshes of the models created using the CAD software Gambit 2.2 (ANSYS, Inc., Canonsburg, PA, USA) were all unstructured hexahedron grid. The commercially available computational fluid dynamics code, FLUENT 6.2 (ANSYS, Inc.) was used in the numerical simulation. Discretization of the pressure and momentum at each control volume was in a second-order scheme. The iterative process of computation was terminated when the residual of mass and velocity were all less than the convergence criterion, $1.0 \times 10^{-5}$.

## Results

### *The length of flow disturbance zones*

Figure 4 shows the length ($L$) of the flow recirculation zones distal to the five stent rings indicated in Figure 3 for the three types of stents tested. The averaged value of $L$ for the five flow recirculation zones ($\bar{L} = \sum_{i=1}^{5} L_i/5d$) is illustrated in Figure 4(C). As evident from the figure, for both Reynolds numbers, the streamlined cross-sectional stent has much smaller disturbed flow zones than the clinical metal stents. More interestingly, as shown in Figure 4(C), opposite to the clinical metal stents, the average length of the disturbed flow zones in the streamlined stent decreases when *Re* increases from 180 to 360.

### *WSS distribution*

Figure 5 shows the distribution of the area-averaged WSS ($\overline{\mathrm{WSS}}$) and their total averaged value ($\overline{\mathrm{WSS}}' = \sum_{i=1}^{5} \overline{\mathrm{WSS}}_i/5$) (Figure 5(C)) over the five flow recirculation zones under different experimental conditions. As evident from the figure, WSS in the test tube with the streamlined stent rings is almost the same as the value in the tube without stent rings, and is much higher than the value in the tube with the clinical metal stent rings.

### *Adhesion of U-937 cells*

Figure 6 is the plot of averaged U-937 cell adhesion density ($Q$) in each disturbed flow zone of the test tube and their total averaged value ($Q' = \sum_{i=1}^{5} Q_i/5$) (Figure 6(C)). The figure shows that U-937 cell adhesion density in the test tube with the streamlined stent rings is only slightly higher than that in the tube without stent rings, but much lower than the cell adhesion densities in the tubes with the

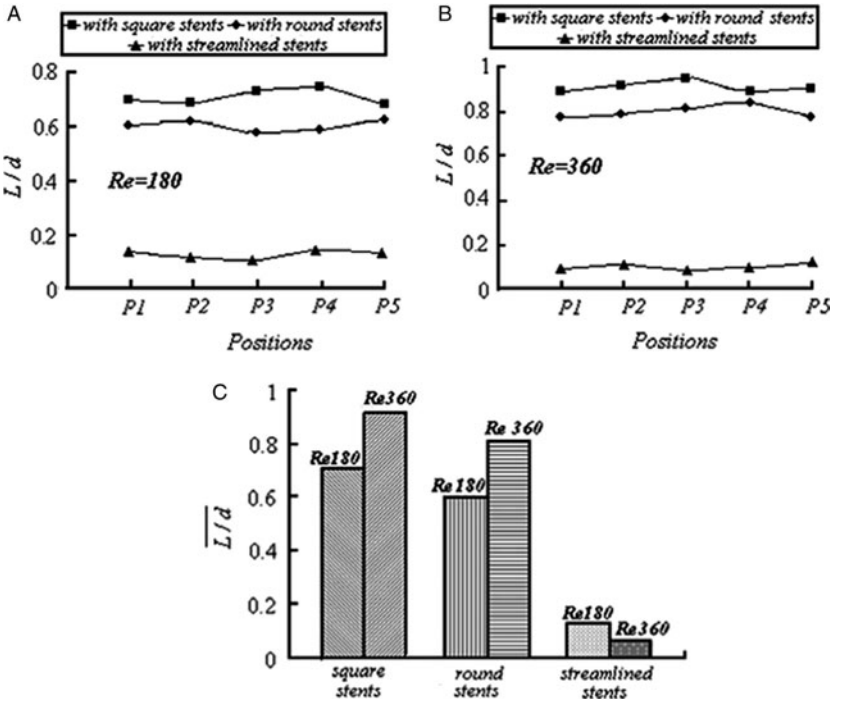


Figure 4. Effect of cross-sectional shape of the stent rings on the length of flow recirculation zones. *P*1 to *P*5 denote the recirculation zone distal to each stent ring indicated in Figure 3. (A) $Re = 180$; (B) $Re = 360$; (C) averaged length of the five flow recirculation zones.

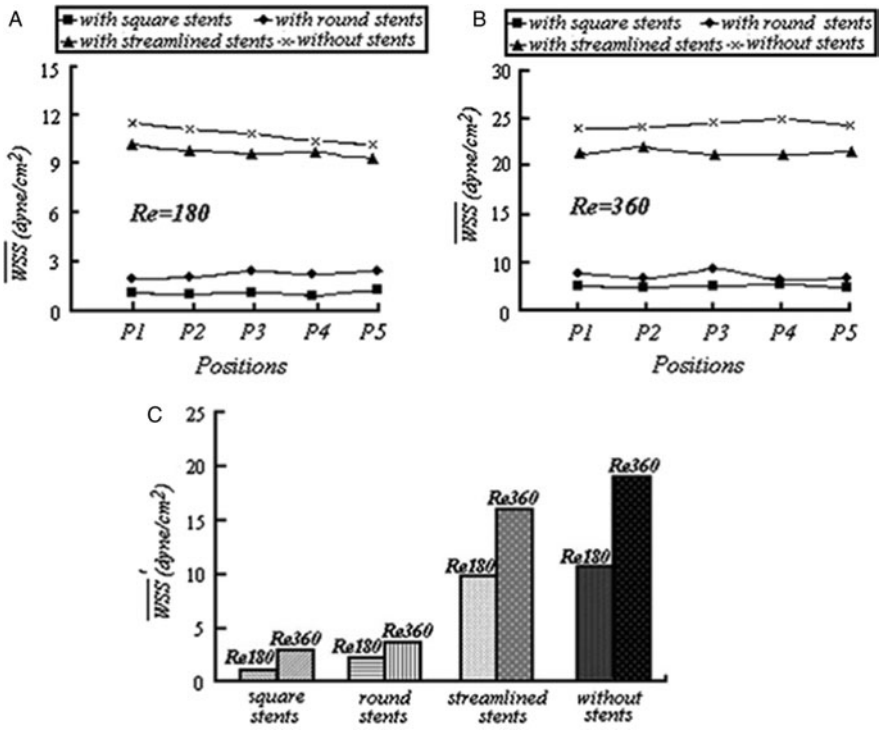


Figure 5. Effect of cross-sectional shape of the stent rings on the area-averaged WSS ($\overline{WSS}$) in the flow recirculation zones. $P1$ to $P5$ denote the recirculation zone distal to each stent ring indicated in Figure 3. (A) $Re = 180$; (B) $Re = 360$; (C) total averaged value of WSS over the five flow recirculation zones.

clinical metal stent rings ($P < 0.05$). Furthermore, as evident from the figure, the cell adhesion density in the test tubes with the clinical metal stents increased when *Re* increased from 180 to 360, while it reduced in the test tube without stent rings or with the streamlined stent rings.

## Discussion

Endovascular stent restenosis has been considered as the most significant drawback in coronary interventional treatments (Dangas and Fuster 1996). Experimental studies have revealed that stent configuration influences intimal hyperplasia and restenosis rate (Tominaga et al. 1992; Rogers and Edelman 1995; Kolandaivelu et al. 2011). Therefore, structural optimization should take a high priority in the design of endovascular stents in order to improve their hemodynamic performance that has been recognized to have a close correlation with the development of restenosis (Liu et al. 2002). Adhesion of monocytes is an important issue for the development of stenting restenosis and can be enhanced significantly by local disturbed blood flow with low WSS (Barber et al. 1998; Chiu and Chien 2011). Therefore, suppressing monocyte adhesion by minimizing flow disturbance in a stent might be one of the solutions to the restenosis problem of endovascular stenting.

In the present paper, we proposed to construct the stents with streamlined cross-sectional wires in a belief that the streamlined stent can minimize disruptions to blood flow so that monocyte adhesion can be reduced in the stent.

To test the hypothesis, we designed a comparative experimental study in which U-937 cell adhesion was observed along test tubes with clinical metal stents or the new concept one implanted. The results showed that by using streamlined cross-sectional wires, the flow disturbance zone distal to each wire ring of the stent could be significantly suppressed so that the adhesion of U-937 cells in the test tube with the new stent was much less than those in the test tubes with the clinical metal stents (the square or round cross-section stents).

More interestingly, the numerical flow simulation revealed that unlike the clinical metal stents, the sizes of the disturbed flow zones distal to the new stent rings did not increase but reduced when *Re* increased from 180 (the rest condition for the coronary arteries) to 360 (the strenuous exercise condition for the coronary arteries). Because the larger the sizes of the disturbed flow zones, the longer the cells would stagnate in the disturbed flow zones, which would lead to higher cell adhesion, the new concept stent is more advantageous over the clinical metal stents under strenuous exercise conditions for the coronary arteries. Therefore, we believed that if this new stent with

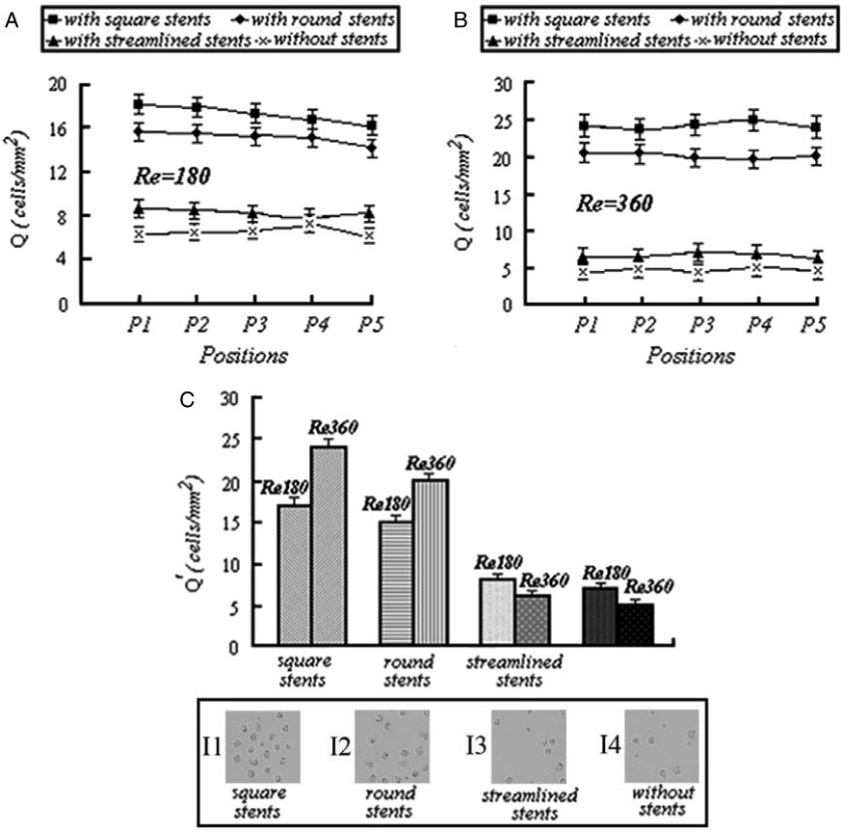


Figure 6. Effect of cross-sectional shape of the stent rings on U-937 cells adhesion density in the five flow recirculation zones ($P < 0.05$). $P1$ to $P5$ denote the recirculation zone distal to each stent ring indicated in Figure 3. (A) $Re = 180$; (B) $Re = 360$; (C) total averaged value of U-937 cells adhesion density over the five flow recirculation zones. The I1, I2, I3 in the bottom rectangle exhibit the adhering cells in a square millimeter at in the disturbed zone of $P5$ after stents with different cross-sectional shapes under the low $Re$ of 180 and I4 in the bottom rectangle shows adhering cells in a square millimeter as the comparing condition without stent.

streamlined cross-sectional wires could be used in clinical treatment, it might reduce the probability of restenosis happening for it had good performance in suppressing the flow disturbance and reducing the adhesion of monocytes.

## Conclusion

In conclusion, the present experimental study suggests that the optimization of the cross-sectional shape of stent wires ought to be taken into consideration in the design of endovascular stents.

## Funding

The project was supported by grants in aid from the National Science Foundation of China [31170904, 11072023, 11172156, 30970822 and 11202016], the China Postdoctoral Science Foundation funded project [grant no. 2012M510021] and the Special Financial Grant from the China Postdoctoral Science Foundation [grant no. 2013T60105].

## Conflict of interest

The authors declare that there is no conflict of interests regarding the publication of this article.

## Note

1. Both authors contributed equally to this work.

## References

Balossino R, Gervaso F, Migliavacca F, Dubini G. 2008. Effects of different stent designs on local hemodynamics in stented arteries. J Biomech. 41(5):1053–1061.

Barber KM, Pinero A, Truskey GA. 1998. Effects of recirculating flow on U-937 cell adhesion to human umbilical vein endothelial cells. Am J Physiol. 275:591–599.

Beekhuizen H, Verdegaal EM, Blokland I, van Furth R. 1992. Contribution of ICAM-I and VCAM-1 to the morphological changes in monocytes bound to human venous endothelial cells stimulated with recombinant interleukin-4 (rlL-4) or rlL-la. Immunology. 77:468–472.

Benard N, Coisne D, Donal E, Perrault R. 2003. Experimental study of laminar blood flow through an artery treated by a

stent implantation: characterisation of intra-stent wall shear stress. J Biomech. 36(7):991–998.

Berry JL, Santamarina A, Moore, JE, Jr, Roychowdhury S, Routh WD. 2000. Experimental and computational flow evaluation of coronary stents. Ann Biomed Eng. 28:386–398.

Calderon TM, Factor SM, Hatcher VB, Berliner JA, Berman JW. 1994. An endothelial cell adhesion protein for monocytes recognized by monoclonal antibody IG9. Lab Invest. 70:836–849.

Capelli C, Gervaso F, Petrini L, Dubini G, Migliavacca F. 2009. Assessment of tissue prolapse after balloon-expandable stenting. Influence of stent cell geometry. Med Eng Phys. 31:441–447.

Chiu JJ, Chien S. 2011. Effects of disturbed flow on vascular endothelium: pathophysiological basis and clinical perspectives. Physiol Rev. 91:327–387.

Cybulsky MI, Gimbrone, MA, Jr. 1991. Endothelial expression of a mononuclear leukocyte adhesion molecule during atherogenesis. Science. 251:788–791.

Dangas G, Fuster V. 1996. Management of restenosis after coronary intervention. Am Heart J. 132:428–436.

Farb A, Sangiorgi G, Carter AJ, et al. 1999. Pathology of acute and chronic coronary stenting in humans. Circulation. 99:44–52.

Garasic JM, Edelman ER, Squire JC, Seifert P, Williams MS, Rogers C. 2000. Stent and artery geometry determine intimal thickening independent of arterial injury. Circulation. 101:812–818.

Gonzales RS, Wick TM. 1996. Hemodynamic modulation of monocytic cell adherence to vascular endothelium. Ann Biomed Eng. 24:382–393.

Gurbel PA, Callahan KP, Malinin AI, Serebruany VL, Gillis J. 2002. Could stent design affect platelet activation? Results of the platelet activation in stenting (PAST) study. J Invasive Cardiol. 14:584–589.

Hara H, Nakamura M, Palmaz JC, Schwartz RS. 2006. Role of stent design and coatings on restenosis and thrombosis. Adv Drug Deliv Rev. 58(3):377–386.

Hauser IA, Johnson DR, Madri JA. 1993. Differential induction of VCAM-1 on human iliac venous and arterial endothelial cells and its role in adhesion. J Immunol. 151:5172–5185.

Henry PD, Chen CH. 1993. Inflammatory mechanisms of atheroma formation, influence of fluid mechanics and lipid-derived inflammatory mediators. Am J Hypertens. 6:328S–334S.

Hsiao HM, Chiu YH, Lee KH, Lin CH. 2012. Computational modeling of effects of intravascular stent design on key mechanical and hemodynamic behavior. Comput-Aided Des. 44(8):757–765.

Hsiao HM, Lee KH, Liao YC, Cheng YC. 2012. Hemodynamic simulation of intra-stent blood flow. Procedia Eng. 36:128–136.

Kastrati A, Mehilli J, Dirschinger J, et al. 2001. Restenosis after coronary placement of various stent types. Am J Cardiol. 87:34–39.

Kolandaivelu K, Swaminathan R, Gibson WJ, Kolachalama VB, Nguyen-Ehrenreich KL, Giddings VL, Coleman L, Wong GK, Edelman ER. 2011. Stent thrombogenicity early in high-risk interventional settings is driven by stent design and deployment and protected by polymer-drug coatings. Circulation. 123(13):1400–1409.

LaDisa, Jr, JF, Olson LE, Guler I, et al. 2005. Circumferential vascular deformation after stent implantation alters wall shear stress evaluated with time-dependent 3D computational fluid dynamics models. J Appl Physiol. 98:947–957.

Lansky AJ, Roubin GS, O'Shaughnessy CD, et al. 2000. Randomized comparison of GR-II stent and Palmaz–Schatz stent for elective treatment of coronary stenoses. Circulation. 102:1364–1368.

Liu SQ, Zhong L, Goldman J. 2002. Control of the shape of a thrombus-neointima-like structure by blood shear stress. J Biomech Eng. 124:30–36.

Mattos MA, Hodgson KJ, Hurlbert SN, et al. 1999. Current problems in surgery. Curr Probl Surg. 36:909–1053.

McLean DR, Eigler NL. 2002. Stent design: implications for restenosis. Rev Cardiovasc Med. 5:S16–S22.

Moreno PR, Bernardi VH, Lopez-Cuellar J. 1996. Macrophage infiltration predicts restenosis after coronary intervention in patients with unstable angina. Circulation. 94:3098–3102.

Morton AC, Crossman D, Gunn J. 2004. The influence of physical stent parameters upon restenosis. Pathol Biol. 52:196–205.

Ng CK, Deshpande SS, Irani K, Alevriadou BR. 2002. Adhesion of flowing monocytes to hypoxia-reoxygenation-exposed endothelial cells: role of Rac1, ROS, and VCAM-1. Am J Physiol Cell Physiol. 283:C93–102.

Papafaklis MI, Chatzizisis YS, Naka KK, Giannoglou GD, Michalis LK. 2012. Drug-eluting stent restenosis: effect of drug type, release kinetics, hemodynamics and coating strategy. Pharmacol Ther. 134(1):43–53.

Pritchard WF, Davies PF, Derafshi Z, et al. 1995. Effects of wall shear stress and fluid recirculation on the localization of circulating monocytes in a three-dimensional flow model. J Biomech. 28:1459–1469.

Rogers C, Edelman ER. 1995. Endovascular stent design dictates experimental restenosis and thrombosis. Circulation. 91:2995–3001.

Rogers C, Edelman ER, Simon DI. 1998. A mAb to the beta2-leukocyte integrin Mac-1 (CD11b/CD18) reduces intimal thickening after angioplasty or stent implantation in rabbits. Proc Natl Acad Sci. 95:10134–10139.

Rogers C, Welt FG, Karnovsky MJ, Edelman ER. 1996. Monocyte recruitment and neointimal hyperplasia in rabbits: coupled inhibitory effects of heparin. Arterioscler Thromb Vasc Biol. 16:1312–1318.

Schmid-Schonbein GW. 1987. Rheology of leukocytes. In: Skalak R, Chien S, editors. Handbook of bioengineering. Vol. 13. New York: McGraw-Hill; p. 1–25.

Seo T, Schachter LG, Barakat AI. 2005. Computational study of fluid mechanical disturbance induced by endovascular stents. Ann Biomed Eng. 33:444–456.

Sigwart U, Puel J, Mirkovitch V, Kappenberger L. 1987. Intravascular stents to prevent occlusion and restenosis after transluminal angioplasty. N Engl J Med. 316:701–706.

Sundström C, Nilsson K:. 1976. Establishment and characterization of a human histiocytic lymphoma cell line (U-937). Int J Cancer. 17:565–577.

Thury A, Wentzel JJ, Vinke RV, Gijsen FJ, Schuurbiers JC, Krams R, de Feyter PJ, Serruys PW, Slager CJ. 2002. Focal in-stent restenosis near step-up: roles of low and oscillating shear stress. Circulation. 105:e185–e187.

Tominaga R, Kambic HE, Emoto H, Harasaki H, Sutton C, Hollman J. 1992. Effects of design geometry of intravascular endoprostheses on stenosis rate in normal rabbits. Am Heart J. 123:21–28.